

Recent Large Earthquakes in India: Seismotectonic Perspective

J.R. Kayal

Jadavpur University, Kolkata - 700 032, India, E-mail: jr_kayal@hotmail.com

Abstract

During the last two decades, seven devastating earthquakes, chronologically, the 1991 Uttarkashi earthquake (m_b 6.6) in the western Himalaya, the 1993 Killari (m_b 6.3) and the 1997 Jabalpur earthquakes (m_b 6.0) in the central part of peninsular India shield area, the 1999 Chamoli earthquake (m_b 6.3) again in the western Himalaya, the 2001 Bhuj earthquake (M_w 7.7) in the western part of peninsular shield area, the 2004 Sumatra-Andaman mega thrust tsunami earthquake (M_w 9.3) in the Andaman-Sunda arc and the 2005 Kashmir earthquake (M_w 7.8) in the western Himalaya syntaxis zone, caused severe damages and large casualties in various parts of India. The 1993 Killari, 1997 Jabalpur and the 2001 Bhuj earthquakes are the Stable Continental Region (SCR) earthquakes in peninsular India, the 1991 Uttarkashi, the 1999 Chamoli and the 2005 Kashmir earthquakes are the Himalayan collision zone earthquakes, and the 2004 Sumatra-Andaman earthquake is one of the four mega thrust earthquakes of the world in the Andaman-Sumatra subduction zone. All these earthquake sequences were well studied by various national and international organizations; the aftershocks were recorded making temporary seismic networks. These investigations have been very useful to understand seismotectonics of the SCR events and the collision zone and subduction zone events of the Indian subcontinent.

Keywords: Stable continental region, collision zone, subduction zone, seismotectonics, aftershocks.

Introduction

Peninsular India constitutes one of the most prominent and largest Precambrian shield areas of the world. It is exposed to the south of the Indo Gangetic Alluvial Plains (IGAP); in other words, the IGAP separates the Himalayas to the north and the peninsular India to the south. While the Himalaya is a region of dominant compressional tectonics and the IGAP is a region of relatively less eventful recent sedimentation, peninsular India, in contrast, is a region marked by Early Archaean cratonisation with associated Proterozoic belts; the cratons are separated by 'rifts' (Mahadevan, 1994). The major prominent rifts, which separate the northern and southern blocks of the shield, are the Narmada Son Lineament (NSL) and the Tapti Lineament (TL), together called the SONATA (Son-Narmada-Tapti Lineament) Zone. It is about 1000 km long and 50 km wide in the central part of India (Fig. 1). The other prominent rift is the Kutch rift at the northwest margin of the Indian shield. It was reported that the seismicity of peninsular India is low despite its ongoing collision with Central Asia (Chandra, 1977). During the last decade, however, three strong/large earthquakes (M 6.0~7.7) occurred in peninsular India: the 1993 Killari earthquake in the southern block of the shield, the 1997 Jabalpur earthquake in the central SONATA zone and the

2001 Bhuj earthquake in the Kutch rift basin, in the western part of the shield (Fig. 1).

To the north, the Himalaya is the greatest mountain chain in the world, about 2500 km long, extending from Kashmir in the northwest to Arunachal Pradesh in the northeast, evolved as a consequence of collision of the Asian and Indian continents some 50 m.y. ago (Valdiya, 1984). The major thrust/fault systems spanning the entire length of the Himalayan arc, from north to south, are: the Indus Suture Thrust (IST), the Main Central Thrust (MCT), the Main Boundary Thrust (MBT) and the Himalayan Frontal Thrust (HFT), and the seismicity between the MCT and MBT is defined as the Main Himalayan Seismic Belt (MHSB). Many large ($M > 7.0$) and great earthquakes (M 8.0 and above) occurred in this belt (Kayal, 2001). During the last decade, two strong earthquakes ($M > 6.0 < 7.0$) occurred in the western Himalaya tectonic zone, the 1991 Uttarkashi and the 1999 Chamoli earthquakes.

The Himalayan arc joins the Burma-Andaman-Sumatra-Sunda arc to the southeast, that defines a ~5,500 km long boundary between the Indo-Australian and Eurasian plates from Myanmar (Burma) to Sumatra and Java to Australia (Curry et al., 1979). Global reconstructions suggest that the Indian plate converges obliquely toward the Asian plate at a rate of 54 mm/year

(DeMets et al., 1994). The Andaman-Sumatra section of the subduction zone has produced many large earthquakes in the past, some of which have also generated destructive tsunamis (Bilham et al., 2005). The M_w 9.3, December 26, 2004 earthquake is the largest to have occurred in this zone; it ruptured more than 1300 km length of the arc in the north direction, from Sumatra to Andaman island, which included segments that were ruptured by the past large earthquakes.

The above-mentioned six devastating earthquakes, the 1991 Uttarkashi, 1993 Killari, 1997 Jabalpur, 1999 Chamoli, 2001 Bhuj, and the 2004 Sumatra, that occurred during last two decades are well studied by monitoring aftershocks by immediate deployment of temporary microearthquake networks. The results of these aftershock investigations, which have been already reported and

published by several authors, are highlighted here. These earthquakes occurred in three tectonic zones of the Indian subcontinent, Stable Continental (SCR) zone, Himalayan Collision Zone and the Andaman-Sumatra Subduction Zone. The aftershock investigations shed some new light on our understanding of the earthquake generating processes in these three distinct tectonic zones of the subcontinent.

SCR Earthquakes in Peninsular India

The 1993 Killari Earthquake (m_b 6.3)

The September 30, 1993 Killari earthquake (m_b 6.3) occurred in the Deccan province of Central India (Fig. 1); the maximum intensity VIII was estimated (Fig. 2). The main shock parameters were reported by the global as

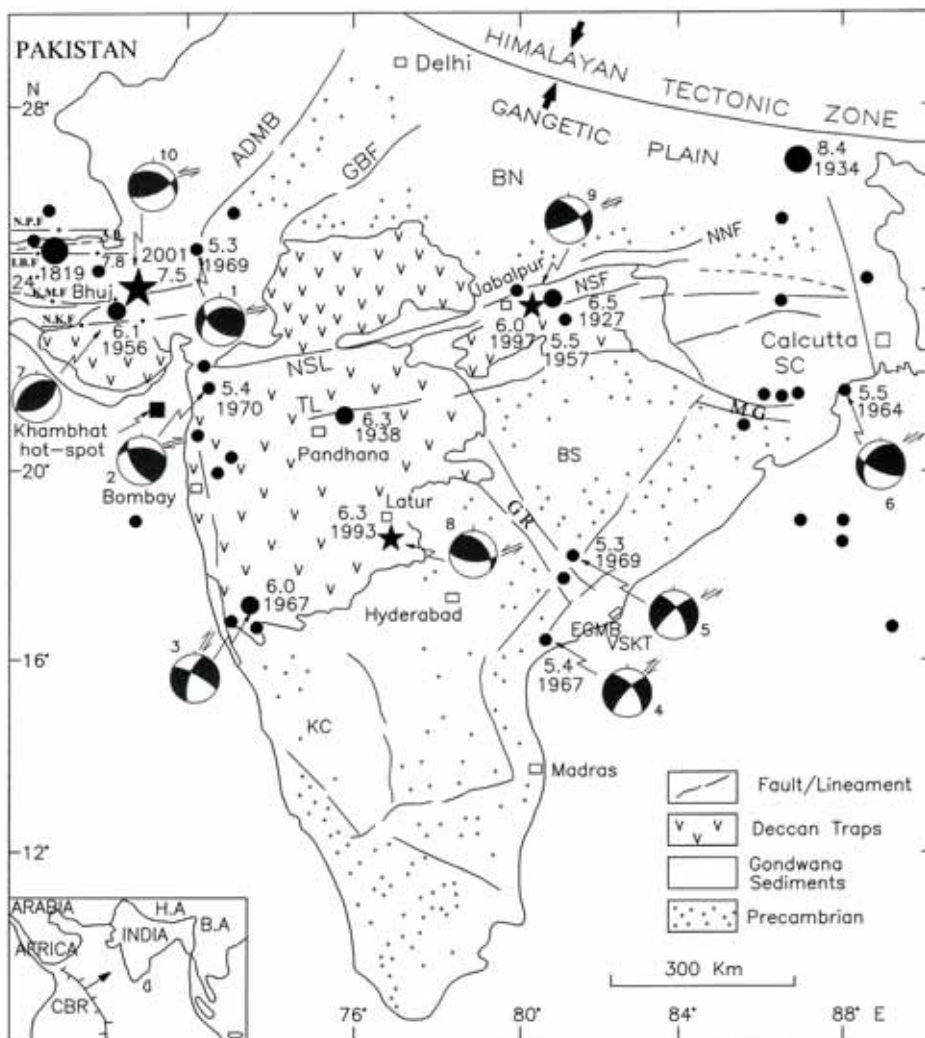


Fig. 1. Map showing seismotectonic domains in peninsular India and the significant earthquakes with fault plane solutions, the three strong earthquakes that occurred during the last decade are indicated by the star symbols. ADBM–Aravalli Delhi Mobile Belt, GBF–Great Boundary fault, NSL–Narmada Son Lineament, NNF–Narmada North Fault, NSF–Narmada South Fault, TL–Tapti Lineament, EGMB–Eastern Ghat Mobile Belt, GR–Godavari Rift, MG–Mahanadi Graben, BN–Bundelkhund, SC–Singhbhum Craton, BS–Bastar Craton, KC–Karnataka Craton (Kayal, 2000). Inset: Key map showing the NNE movement of the Indian plate, CBR–Carlsberg Ridge, HA–Himalayan Arc, BA–Burmese Arc.

well as by the national network. The aftershocks were monitored by temporary networks (Kayal, 2000; Baumbach et al., 1994). The main shock and its 150 well located aftershocks ($M > 2.0$) were confined to a shallower depth (0–15 km), the sequence is a typical example of common type of SCR earthquakes (Kayal, 2000).

The main shock occurred by reverse faulting at a depth of 6 km; the deeper (6–15 km) aftershocks also occurred by reverse faulting (Fig. 2a). The shallower aftershocks, (0–<6 km), on the other hand, occurred by right-lateral strike-slip faulting. The area is covered by Deccan traps, no surface geological fault was mapped. Fault plane solutions (Fig. 2a) and seismic cross-section of the main shock and deeper aftershocks (Fig. 2b), however, suggest a south dipping E-W fault that corroborates with the E-W Tirna River in the main shock epicentre area. The fault

plane solution of the shallower (0–<6 km) aftershocks, on the other hand, shows a NW-SE trending strike slip fault that corroborates with the Tirna tributary (Fig. 2a). The earthquake sequence is explained by a fault interaction model (Fig. 2c).

Seismic tomography study revealed a detailed velocity structure of the earthquake source area (Kayal and Mukhopadhyay, 2002). The seismic image at the 6 km depth slice shows that the main shock occurred at the contact of a high velocity zone (HVZ) and a low velocity zone (LVD), (Fig. 3a). The E-W trending LVZ possibly represents the fault zone, and at the “fault end” at a depth of 6 km the main shock occurred within the HVZ (Fig. 3a), the HVZ acted as a stress concentrator (Kayal and Mukhopadhyay, 2002). The E-W trending fault zone (LVZ) is comparable with the E-W trending Tirna River

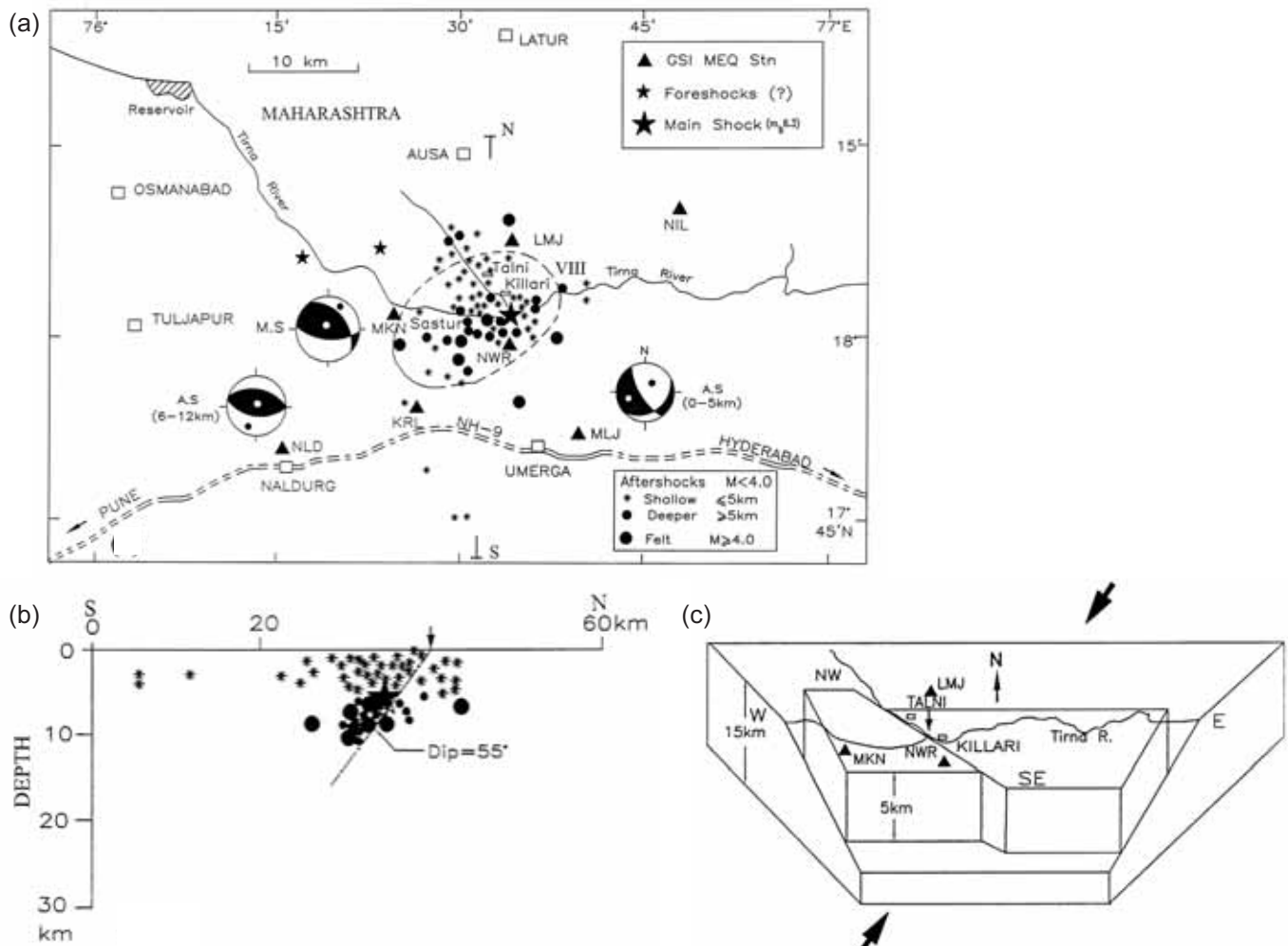


Fig. 2. (a) Map showing isoseismal (intensity VIII) of the 1993 Killari earthquake, temporary microearthquake stations, epicentres of the main shock and aftershocks with fault plane solutions, (b) N-S seismic cross section of the main shock and aftershocks, that shows a south dipping plane for the main shock and the deeper aftershocks and its surface projection meets the surface rupture indicated by a small arrow. (c) Fault interaction model of the Killari earthquake sequence, the main shock and the deeper aftershocks occurred by reverse movement of the upper block and the shallower aftershocks occurred by strike slip movement within the upper block, the small arrow in the upper block indicates the surface rupture. The larger arrows indicate the regional tectonic stress (Kayal, 2000).

on the surface. At the 3 km-depth slice, a NW-SE trending LVZ is observed (Fig. 3b), and the shallower aftershocks follow this trend along the Tirna tributary.

Based on the above observations Kayal (2000) and Kayal and Mukhopadhyay (2002) suggested that intersection of the two faults was the source zone of the Killari earthquakes, and a high velocity zone at the fault end at depth was the source area for the main shock. These fault zones were further evidenced by detailed post earthquake gravity study (Mishra et al., 1994) and by deep drilling (Gupta and Dwivedi, 1996).

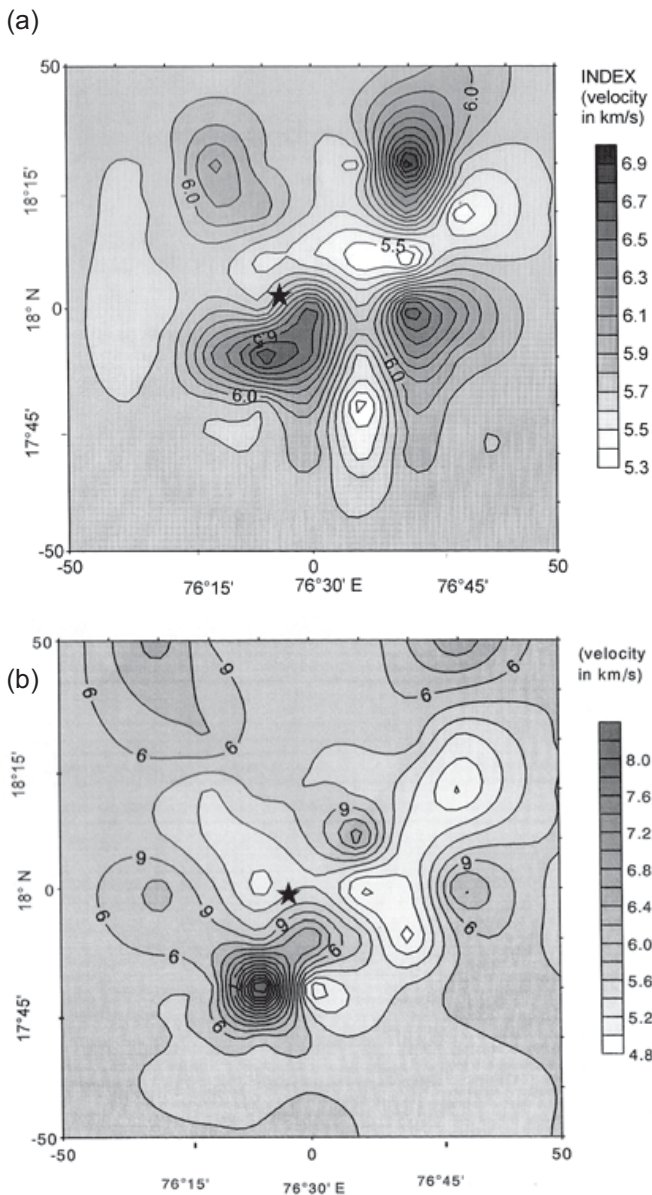


Fig. 3. Seismic tomography of the Killari earthquake source area, (a) at 6 km depth, and (b) at 3 km depth; star indicates the main shock (Kayal and Mukhopadhyay, 2002).

The 1997 Jabalpur earthquake (m_b 6.0)

The May 22, 1997 Jabalpur earthquake (m_b 6.0), maximum intensity VIII, occurred at the base of the Narmada Rift Basin in the SONATA, within the SCR, at a depth of 35 km by reverse faulting with a left-lateral strike-slip motion (Figs.1 and 4a). This is the first significant strong earthquake that was recorded by the broadband stations of the national network, and the focal depth was well estimated using the depth phases (Bhattacharya et al., 1997). Only about 25 aftershocks ($M > 2.0$) were recorded by a temporary network (Kayal, 2000); it may be noted that the main shock and the aftershocks occurred outside the meizoseismal (intensity VIII) zone (Fig. 4a). The fault-plane solution of the aftershocks also reveals reverse faulting with left-lateral strike-slip motion (Fig. 4a). The seismic cross section of the main shock and aftershocks indicates that the south dipping Narmada South Fault

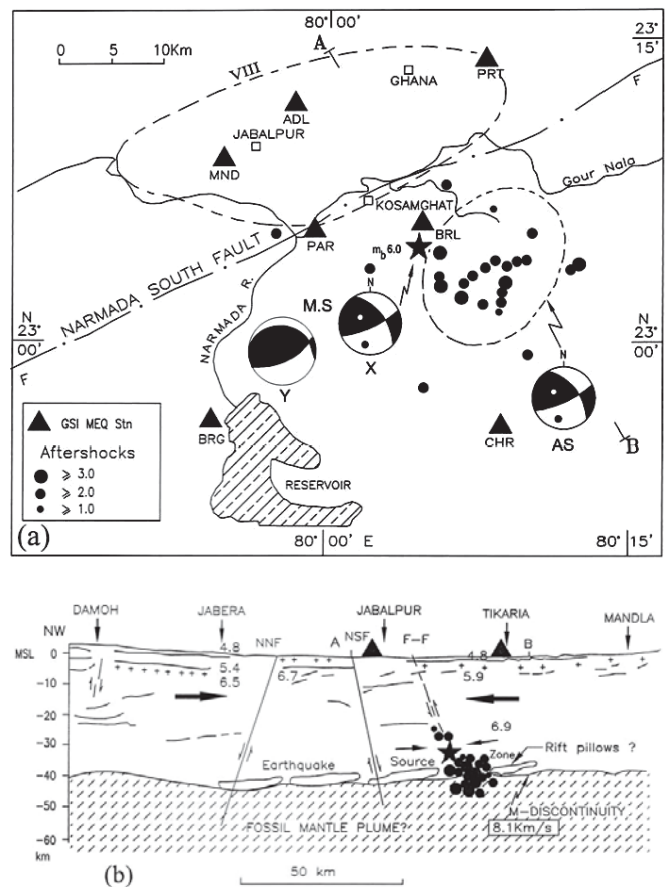


Fig. 4. (a) Map showing meizoseismal area (intensity VIII) of the 1997 Jabalpur earthquake, temporary seismic stations and epicentres of the main shock and aftershocks, and fault plane solutions. Two solutions (X: USGS and Y: IMD) of the main shock (MS) are given; AS represents the composite solution of the aftershocks. (b) Seismic cross-section of the main shock and aftershocks with crustal section of the velocity structure (Kayal, 2000).

(NSF), the southern margin fault of the Narmada Rift Basin, was activated by reverse faulting (Fig. 4b), and the earthquakes occurred at a depth 35–40 km. The seismic section further reveals that the source area in the rift basin was deeper, at the crust-mantle boundary, at the “fault end”. The well studied aftershocks by the close spaced temporary network confirms the deeper source area of the main shock and aftershocks. The observations further suggest that the rift basin boundary faults are mantle reaching; these faults, which were developed by tensional regime and created the rift basin in the geological past, are now under compressive stress due to the NNE movement of the Indian plate. The fault plane solutions of the main shock and the aftershocks indicate consistent NNE-SSW compressive stress (Fig. 4a). Seismic tomography of the source area could not be done due to meagre aftershock data. The aftershock investigation, however, revealed that the NSF is a seismogenic deep fault, and it was well mapped on the surface by the geological evidences (Acharyya et al., 1998). The Jabalpur earthquake is a good example of a deeper paleo-rift basin earthquake in the SCR of peninsular India, and the existing faults of the basin reactivate to generate earthquakes.

The 2001 Bhuj earthquake (M_w 7.7)

The most recent devastating Bhuj earthquake (M_w 7.7) of January 26, 2001 is one of the largest events that

occurred in SCR of the world. The maximum intensity reached X (MSK scale), (Fig. 5). This is the second largest event in the western margin of peninsular India after the 1819 great Kutch earthquake ($M \sim 8.0$). The 2001 Bhuj earthquake is another example of a deeper paleo-rift basin earthquake within the SCR of peninsular India, which occurred at a depth of 25 km in the Kutch Rift Basin. About 1000 aftershocks ($M > 2.0$) were recorded by a temporary network, and about 500 well located epicentres are shown in the map (Fig. 5). The fault-plane solutions of the main shock and the selected aftershocks show complicated earthquake processes, but the NNE-SSW regional compressive stress is consistent for all the solutions (Fig. 6). The seismic sections and the fault plane solutions suggest a fault interaction model (Fig. 7), which illustrates that the main shock originated at the base of the paleo-rift basin by reverse faulting on a deep seated south dipping hidden fault; the rupture propagated along NE as well as along NW. The aftershocks occurred by left-lateral strike-slip motion along the NE trending fault, compatible with the main shock solution, and by pure reverse to right-lateral strike-slip motion along the NW trending conjugate fault; these solutions are not compatible with the main shock solution (Fig. 6). The evidences of ground motion are compatible with the strike slip motions obtained by the fault plane solutions along the two trends (Fig. 7). The model further illustrates that the Kutch Mainland Fault (KMF), which runs E-W in the central part of the

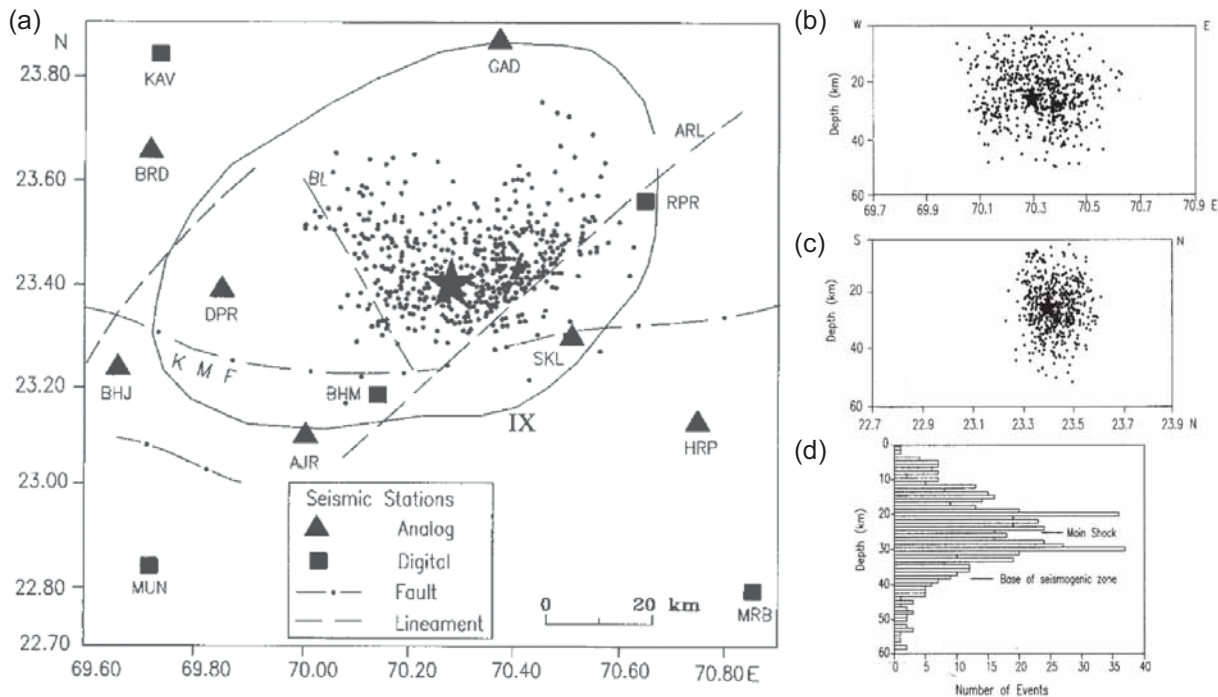


Fig. 5. (a) Relocated Bhuj aftershocks (small dots) by simultaneous inversion, main shock is shown by the solid star, major tectonic features and the high intensity zone are shown. KMF–Kutch Mainland Fault, AR–Anjar-Rapar Lineament, BL–Bhachau Lineament. (b) E-W depth-section and (c) N-S depth-section of the main shock and aftershocks, and (d) frequency of aftershocks at each 1 km depth interval shows a bimodal activity (Kayal and Mukhopadhyay, 2006).

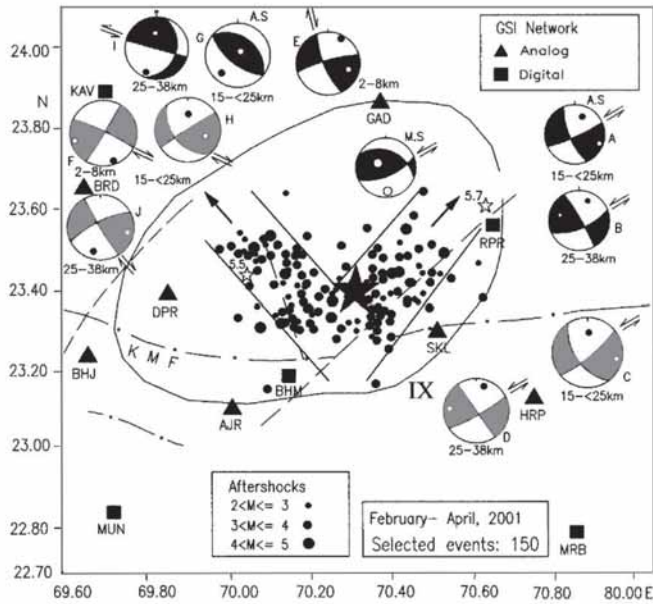


Fig. 6. Fault plane solutions of the main shock (MS) and selected aftershocks (AS) are shown with usual notations, the darker solutions are for the February 2001 sequence and the solutions with lighter shades for the March-April 2001 sequence, two largest aftershocks (M 5.7 and 5.5) are shown by open stars, two trends of seismicity are marked (Kayal et al., 2002a and Kayal and Mukhopadhyay, 2006).

basin, is not the causative fault for the Bhuj earthquake sequence; a steeply south dipping hidden fault which did not rupture to the surface generated the main shock at deeper depth, and the rupture propagated to the NE and NW at depth to generate the aftershocks. The seismic data further illustrates a bimodal activity of the aftershocks (Fig. 5d), and the aftershocks mostly occurred at a depth 15–35 km.

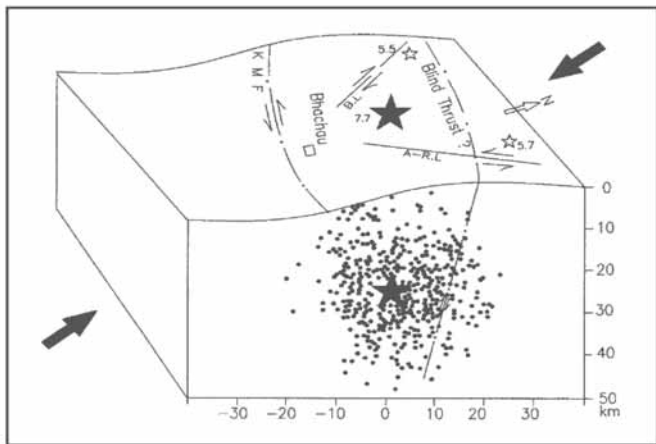


Fig. 7. Seismotectonic model of the 2001 Bhuj earthquake sequence, depth section of the events are taken from figure 5c, solid arrows indicate the regional tectonic stress. Observed ground motions along the two major lineaments (ARL and BL) are comparable with the fault plane solutions (modified from Kayal et al., 2002a and Kayal and Mukhopadhyay, 2006).

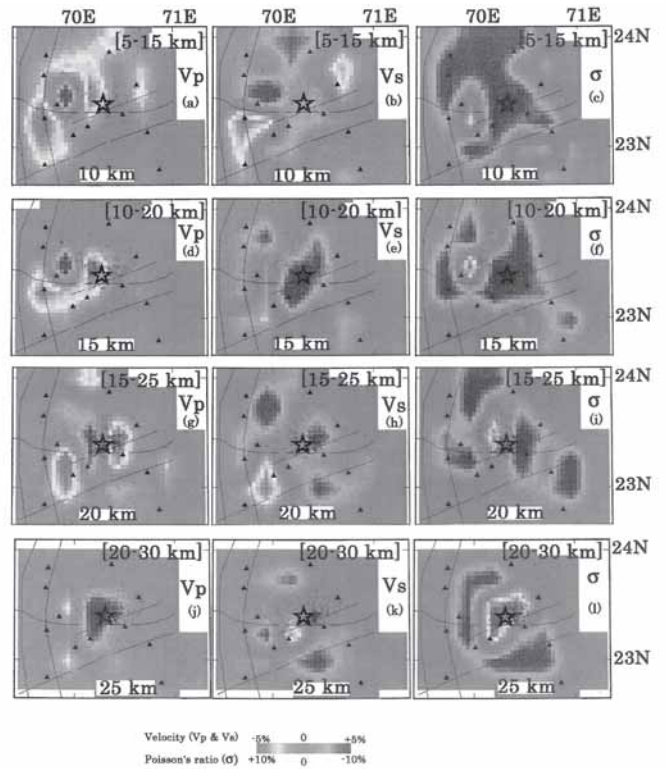


Fig. 8. Seismic images (V_p , V_s and V_p/V_s) of the Bhuj earthquake source area (Kayal et al., 2002b).

Seismic tomography study revealed high V_p , low V_s and high V_p/V_s in the source area at 25 km depth (Fig. 8), which indicate that the source area is a fluid-filled fractured rock matrix that triggered the main shock (Kayal et al., 2002b). The high velocity source zone is bounded by two low velocity zones (LVZs), one to the east and other to the west at 10–20 km; the LVZs possibly indicate the sheared faults/rupture zones. At the “fault ends” lies the high velocity source area at 25 km depth, which acted as a stress concentrator to generate the main shock (Fig. 8); the aftershocks were triggered along the two (LVZs) faults, the fault interaction model (Fig. 7) fits fairly well with the tomography study.

Himalayan Collision Zone Earthquakes

We shall briefly discuss two earthquake sequences in this section, that occurred in the western Himalaya collision zone, the 1991 Uttarkashi and the 1999 Chamoli earthquakes. These two strong events ($7 > M > 6$), that caused severe damages in the area, occurred in the so called central gap between the two great earthquake rupture zones, 1905 Kangra earthquake ($M \sim 8.0$) and the 1934 Bihar earthquake ($M \sim 8.4$), (Fig. 9).

The 1991 Uttarkashi Earthquake (m_b 6.6)

The Uttarkashi earthquake (m_b 6.6) of October 20, 1991

occurred in a complicated tectonic setting in the western Himalayan collision zone. The maximum intensity of the earthquake was estimated IX (MSK scale) in an area of 20 sq km in the epicentre zone (Fig. 10a). This is the first strong event in the Himalaya which was well studied by a temporary network, about 125 aftershocks ($M > 2$) were well located (Fig. 10a). The main shock occurred at a depth of 15 km and the aftershocks occurred at 0–15 km depth. The fault plane solution of the main shock shows a low angle thrust faulting, and the aftershocks show a reverse faulting (Fig. 10a). The seismic section of the main shock and the aftershocks fits fairly well with the conceptual tectonic model of the western Himalaya envisaged by Seeber et al. (1981) and Ni and Barazangi (1984). The main shock and all the aftershocks occurred on and above the Plane of Detachment (Fig. 10b). The north-dipping nodal plane of the fault plane solution of the main shock corroborates well with the low angle north dipping basement thrust or Plane of Detachment, and the steeply north dipping nodal plane of the composite fault plane solution of the aftershocks corroborates well with the dip of the Uttarkashi fault that merges on the Plane of Detachment at depth (Fig. 10b).

The 1999 Chamoli Earthquake (m_b 6.3)

The March 28, 1999 Chamoli earthquake (m_b 6.3), maximum intensity VIII, occurred by thrust faulting at a shallower depth (21 km) in the western Himalaya, epicentre lies about 100 km southeast of the 1991 Uttarkashi earthquake (Fig. 9). The maximum intensity

is bounded by the Main Central Thrust (MCT) to the north and by the Alokanda Fault (ANF) to the south. About 1000 aftershocks were well recorded by the permanent as well as by the temporary network; well located aftershocks $M > 2.5$ are shown in figure 11a. Seismic section of the main shock and the aftershocks shows that the main shock occurred on the Plane of Detachment, basement thrust zone, where the ANF ends, and the main shock activate the ANF to generate the aftershocks. It may also be noted that like that of the 1991 Uttarkashi earthquake sequence, the Chamoli earthquake sequence is not only confined above the Plane of Detachment, but also occurred to the south of the MCT zone (Fig. 11b). The conceptual tectonic model of the western Himalaya fits fairly well with the observation. Seismic tomography revealed the seismogenic high velocity structure at the earthquake source area, at the “fault end” of the ANF (Fig. 12). The ANF as well as the MCT is well reflected as low velocity zones in the seismic images (Fig. 12).

Andaman-Sumatra Subduction Zone Earthquakes

The 2004 Sumatra-Andaman Tsunami Earthquake (M_w 9.3)

The December 26, 2004 Sumatra-Andaman earthquake (M_w 9.3) is the fourth largest event ($M \geq 9.0$) in the world during the last 100 years. It occurred by thrust faulting on the interplate thrust zone of the subducting Indian plate and overriding Burma platelet. The main shock rupture, ~1300 km long, propagated from north of Sumatra to Andaman-Nicobar Islands, the rupture overshoot all the rupture zones of the past large earthquakes in the Andaman-Sumatra arc (Fig. 13). The slow and long rupture of the 2004 mega thrust event generated the Tsunami which killed about 300,000 people. The epicentre of the earthquake is located at 3.9° N and 94.26° E, north of the Sumatra island with a focal depth at 28 km (Fig. 14).

The mega thrust event was followed by an intense aftershock activity spreading over an area extending between 3° – 14° N along the Andaman–Nicobar–Sumatra Island arc. Larger aftershocks ($M > 5.0$) are recorded by the global as well as by the national network (Fig. 14), and several thousand smaller aftershocks ($M > 2.0$) are recorded by making a temporary network in the Andaman-Nicobar islands by the Geological Survey of India (Mishra et al., 2007). The aftershocks are distributed northwards from the epicentre of the main shock suggesting a unilateral rupture propagation. The aftershock area covers a length of about 1300 km and a width of about 200 km, in a ‘banana’ shape (Fig. 13).

This mega seismic event (M_w 9.3) triggered giant tsunamis that devastated the coastal regions of Indonesia,

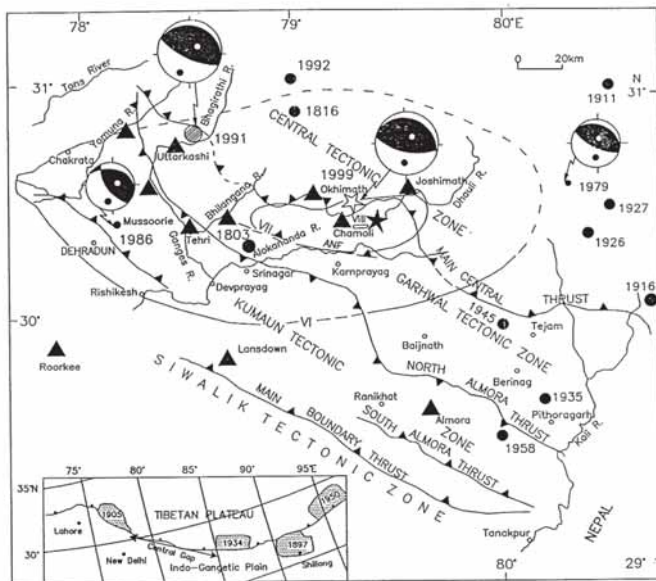


Fig. 9. Seismotectonic map of the western Himalaya showing the major thrust zones, epicentres of the 1991 and the 1999 earthquakes along with the past significant earthquakes and the fault plane solutions in the region (Kayal et al., 2003). Inset: Rupture zones of the great Himalayan earthquakes and the central seismic gap (Khattri and Tyagi, 1983).

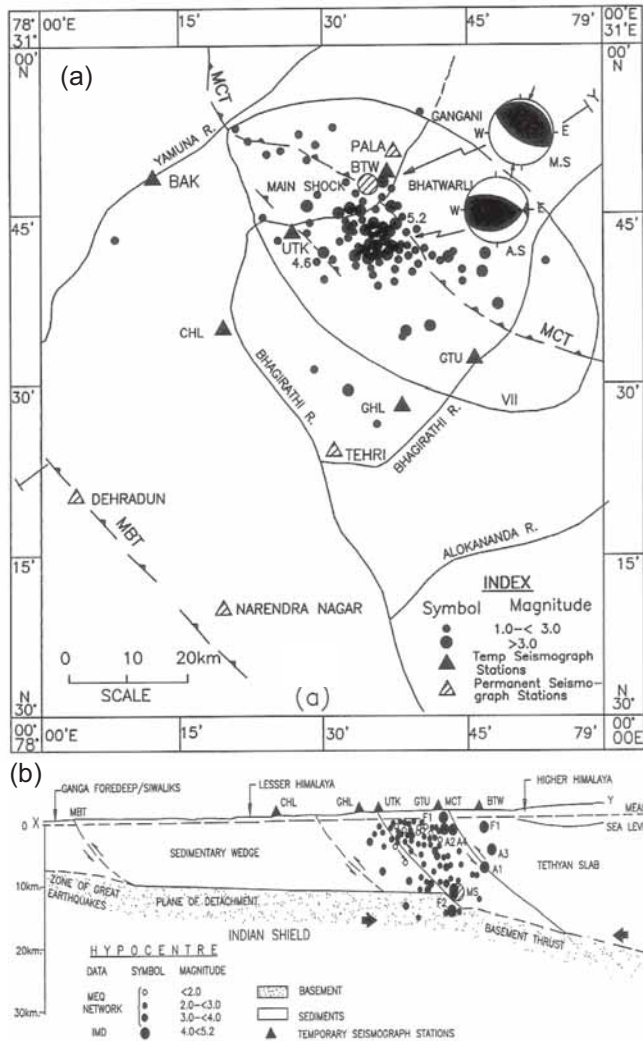


Fig. 10. (a) Map showing the epicentres and fault plane solutions of the 1991 Uttarkashi earthquake and its aftershocks. Isoseismal VII is shown. (b) Seismic section of the main shock and the aftershocks and the tectonic model (Kayal, 1996).

Malaysia, Thailand, Sri Lanka, India, Maldives and even the east coast of Africa. The impact of the tsunami was quite severe in the coasts of Andaman and Nicobar group of Islands, Tamil Nadu, Andhra Pradesh, Pondicherry and Kerala. The airbase in the Car-Nicobar island was totally devastated by the tsunami. Macro seismic survey was carried out by the Geological Survey of India (GSI Unpub. Report, 2005) in North Andaman, Middle Andaman, South Andaman, Havelock, Hut Bay and a maximum intensity VIII was reported in the Andaman Islands. The maximum intensity in the epicentre area was reported to be X (Martin, 2005).

The US Geological Survey (USGS) located about 500 aftershocks $M \geq 4.5$ till January 31, 2005. The GSI deployed six temporary seismograph stations in the Andaman and Nicobar Islands and also in the Narkunda (volcanic) Island. About 20,000 aftershocks ($M \geq 3.0$) were recorded

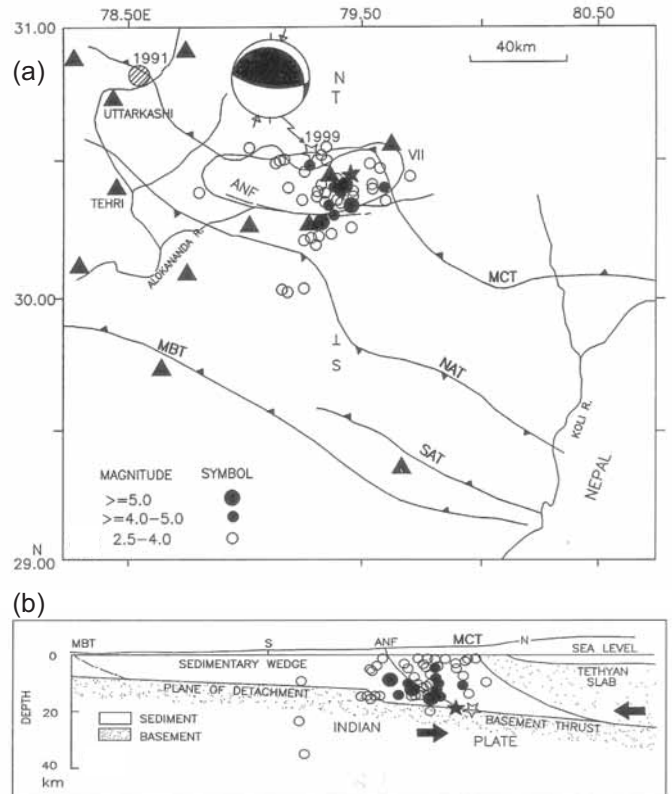


Fig. 11. (a) Aftershock epicentres of the 1999 Chamoli earthquake recorded by temporary network during April 10–June 29, 1999. Fault plane solutions of the main shock (MS) is shown. (b) N-S seismic cross section and seismotectonic model (Kayal et al., 2003).

till end of March, 2005. About 1000 aftershocks ($M \geq 3.0$) are located by the GSI network till January 31, 2005 (Mishra et al., 2007). The aftershocks are still continuing,

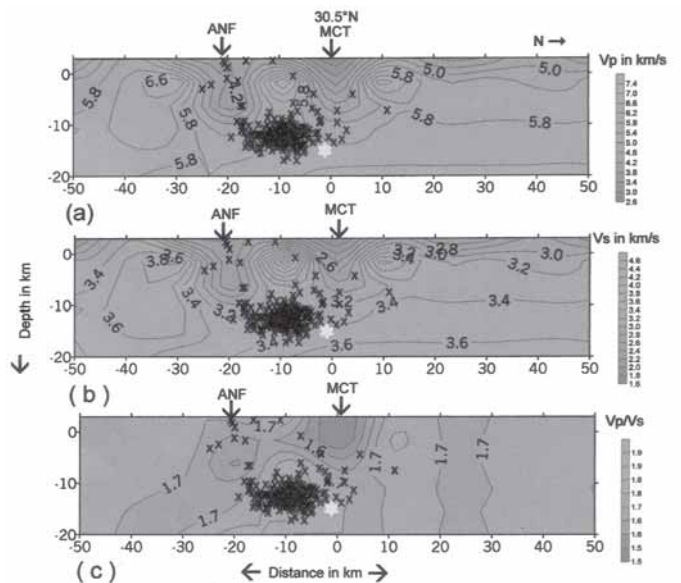


Fig. 12. North-south section of the seismic images (V_p , V_s and V_p/V_s) of the 1999 Chamoli earthquake source area (Mukhopadhyay and Kayal, 2003). The ANF and the MCT are well reflected in the seismic images as low velocity zones.

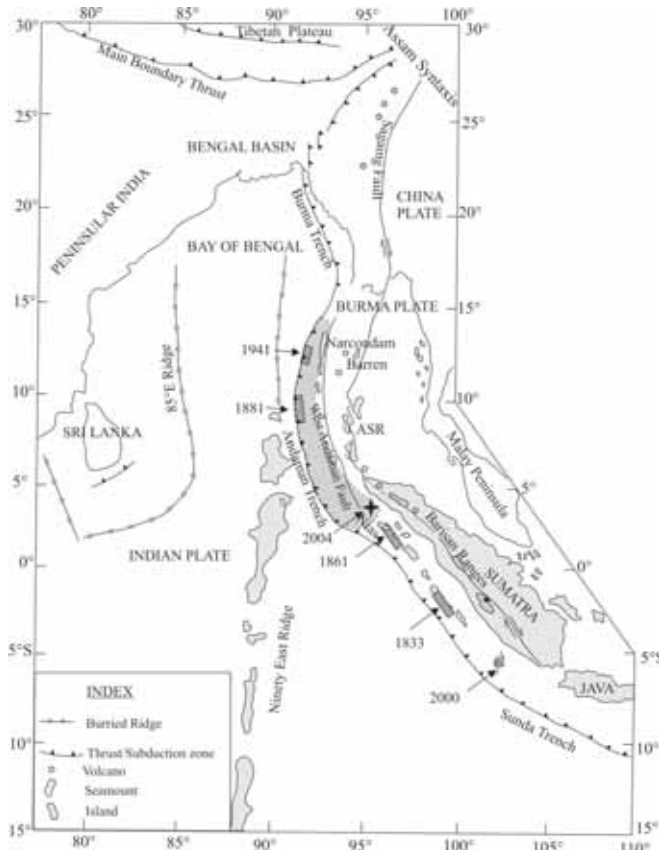


Fig. 13. Tectonic setting of NE India, Indo-Burma ranges and Andaman Sumatra Island arc; rupture zones (darker rectangles) of the past earthquakes and the “banana shape” rupture zone of the 2004 mega thrust event are shown (modified from Kayal et al., 2004).

but frequency of occurrences is, however, much reduced now; aftershocks of such mega thrust event may continue for couple of years to tens of years. The USGS Centroid Moment Tensor (CMT) solutions of the aftershocks suggest predominant thrust faulting in the fore arc region along the West Andaman fault, and normal/strike slip in the back arc region along the Andaman Sea Ridge (ASR) (Fig. 14), consistent with the regional tectonics (Fig. 13). Schematic diagrams are illustrated in figure 15 to explain the fault plane solutions in a subduction zone and associated back arc spreading centre.

The oblique subduction of the Indian plate beneath the Burmese platelet is partitioned into thrust faulting along the plate-interface involving slip directed perpendicular to the trench, and strike-slip faulting much east of the trench with slip directed parallel to the trench axis. A more detailed source structure may be investigated by seismic tomography.

Conclusions

During the last two decades, since 1991, as many as seven strong to mega earthquakes (M 6.0–9.3) severely

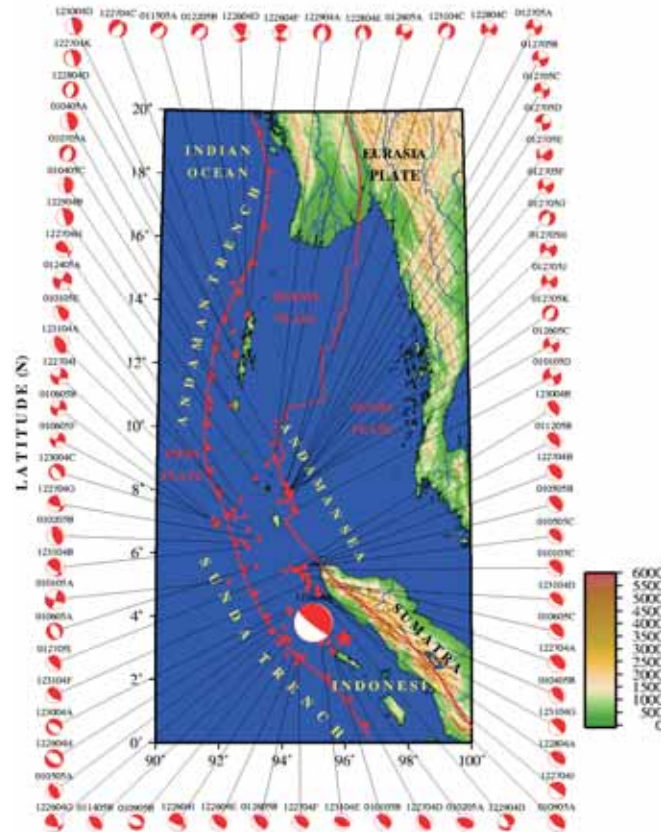


Fig. 14. CMT solutions of the main shock and aftershocks (M>5.0) that were recorded during December 26, 2004–January 31, 2005 by the global network (USGS data source).

rocked the Indian subcontinent causing huge loss of human lives and properties. These earthquakes were well studied by macroseismic and aftershock investigations. The author led aftershock investigations of all the earthquakes except the October 8, 2005 event that occurred in the Kashmir Himalaya, in the western syntaxis zone. Here the results of the six aftershock investigations are highlighted, that shed new light on understanding of the peninsular India SCR, Himalayan collision and Andaman-Sumatra subduction zone earthquake processes.

In the peninsular SCR region we have experienced typical shallow (<10km) shield earthquake (1993 Killari) and deeper (25–35 km) paleo-rift basin (1997 Jabalpur and 2001 Bhuj) earthquakes. The shallow 1993 Killari event produced surface rupture on the otherwise Deccan trap covered area where no surface geological fault is mapped. The 2001 Bhuj earthquake neither produced surface rupture nor occurred on a known surface fault; it was caused by a deep seated hidden fault. The aftershock data were useful for seismic tomography that imaged the heterogeneity of the crustal structure at the source areas for both the 1993 and 2001 events. Fault plane solutions of the aftershocks as well as the seismic images support fault interaction models for these two events. Though a

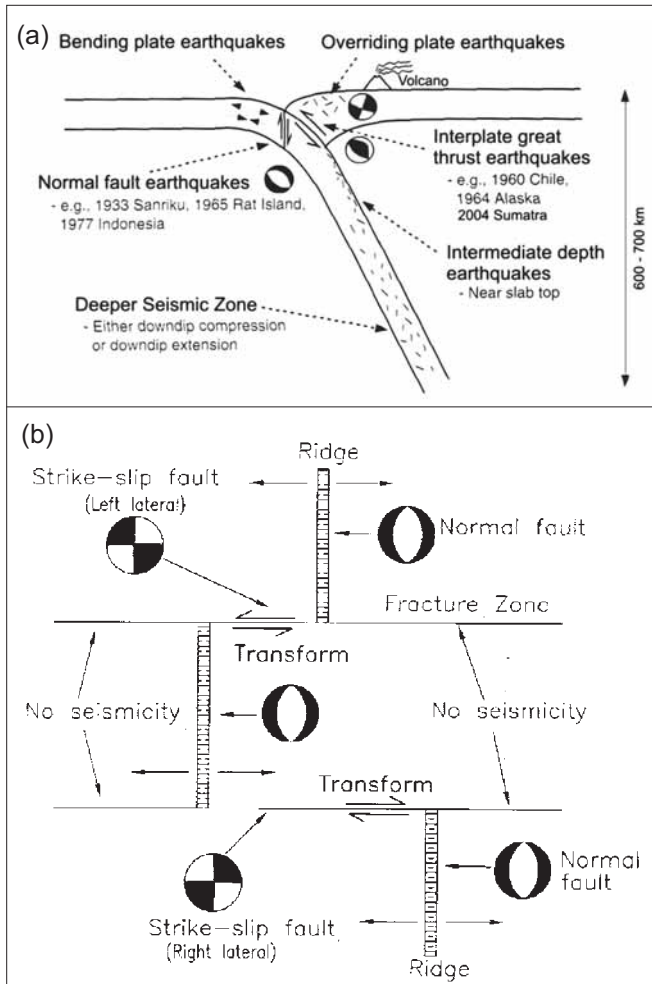


Fig. 15. (a) Schematic illustration of the fault plane solutions in a subduction zone and associated fore arc region, the largest mega thrust events in subduction zones are indicated. (b) Fault plane solutions in an oceanic spreading centre, back arc region (Kayal, 2007).

few aftershocks of the 1997 Jabalpur earthquake were recorded, these data clearly revealed a deeper source of the earthquake at a depth of 35 km at the “fault end” of the paleo-rift basin, the Narmada South fault at the basin margin reactivated to generate the earthquake at the crust mantle boundary.

Both the western Himalayan earthquakes, the 1991 Uttarkashi and the 1999 Chamoli, support the steady state tectonic model of the Himalaya, that suggests that the strong/large earthquakes occur on the Detachment Plane or Basement Thrust at the “fault ends”. The investigations further revealed that the MCT is dormant, the active segments of the faults to the south of MCT are the causative faults for the shallow (0–20 km) Himalayan seismicity.

The 2004 mega thrust event at the Andaman-Sumatra subduction zone is one of the largest subduction zone events ($M > 9.0$) in the world that occurred during the

last century causing devastation and tsunamis. The fault plane solutions of the main shock and aftershocks revealed the complex tectonics of the region. Huge aftershocks are recorded by the global and local seismograph networks; the aftershocks are still continuing. A regional seismic tomography study, which is in progress, would further shed light on the source area of the mega thrust event.

Acknowledgments

This presentation is based on the author’s earlier publications. The kind help of Mr. G. Karunakar and Dr. Devajit Hazarika in graphics is thankfully acknowledged.

References

Acharyya, S.K., Kayal, J.R., Roy, A. and Chaturvedi, R.K. (1998) Jabalpur earthquake of May 22, 1997: constraint from aftershock study. *J. Geol. Soc. India*, v. 51, pp. 295-304.

Baumbach, M., Grosser, H., Schmidt, H.G., Paulat, A., Rietbrock, A., Rao, C.V.R., Raju, P.S., Sarkar, D. and Mohan, I. (1994) Study of the foreshocks and aftershocks of the intraplate Latur earthquake of September 30, 1993, India. *Geol. Soc. India Mem.* No. 35, pp. 33-63.

Bhattacharya, S.N., Ghosh, A.K., Suresh, G., Baidya, P.R. and Saxena, R.C. (1997) Source parameters of Jabalpur earthquake of May 22, 1997. *Curr. Sci.*, v. 73, pp. 855-863.

Bilham, R. (2005) A flying start, then a slow slip. *Science*, v. 308, pp. 1126-1127.

Chandra, U. (1977) Earthquakes of Peninsular India – a seismotectonic study. *Seism. Soc. Amer. Bull.*, v. 67, pp. 1387-1413.

Curry, J.R., Moore, D.G., Lawver, L.A., Emmel, F.J., Raitt, R.W., Henry, M. and Kieckhefer R. (1979) Tectonics of the Andaman Sea and Burma. In: Watkins, J.S., Montadert, L. and Dickenson, P. (Eds.), *Geological and Geophysical Investigation of Continental Margins*. Amer. Assoc. Petrol. Geol. Mem., pp. 189-198.

DeMets, C., Gordan, R.G., Argus, D.F. and Stein, S. (1994) Effect of recent revisions to the geomagnetic reversal time scale on estimates of current plate motions. *Geophys. Res. Lett.*, v. 21, pp. 2191-2194.

Gupta, H.K. and Dwivedi, K.K. (1996) Drilling at Latur earthquake region exposes a peninsular gneiss basement. *J. Geol. Soc. India*, v. 47, pp. 129-131.

Kayal, J.R. (1996) Precursor seismicity, foreshocks and aftershocks of the Uttarkashi earthquake of October 20, 1991 at Garhwal Himalaya. *Tectonophys.*, v. 263, pp. 339-345.

Kayal, J.R. (2000) Seismotectonic study of the two recent SCR earthquakes in central India. *J. Geol. Soc. India*, v. 55, pp. 123-138.

Kayal, J.R. (2001) Microearthquake activity in some parts of the Himalaya and the tectonic model. *Tectonophys.*, v. 339, pp. 331-351.

Kayal, J.R. (2007) *Microearthquake Seismology and Seismotectonics of South Asia*. Capital Pub., New Delhi (in press).

Kayal, J.R. and Mukhopadhyay, S. (2002) Seismic tomography structure of the 1993 Killari earthquake source area, *Seism. Soc. Amer. Bull.*, v. 92, pp. 2036-2039.

- Kayal, J.R. and Mukhopadhyay S. (2006) Seismotectonics of the 2001 Bhuj earthquake (Mw 7.7) in western India: constraints from aftershocks. *J. Indian Geophys. Union*, v. 10, pp. 43-57.
- Kayal, J.R., Gaonkar, S.G., Chakraborty, G.K. and Singh, O.P. (2004) Aftershocks and seismotectonic implications of the 13th September 2002 earthquake (MW 6.5) in the Andaman Sea basin. *Seism. Soc. Amer. Bull.*, v. 94, pp. 326-333.
- Kayal, J.R., De, R., Saginaram, Srirama, B.V. and Gaonkar, S.G. (2002a) Aftershocks of the 26 January, 2001 Bhuj earthquake in western India and its seismotectonic implications. *J. Geol. Soc. India*, v. 59, pp. 395-417.
- Kayal J.R., Sagina Ram, Singh, O.P., Chakraborty, P.K. and Karunakar, G. (2003) Aftershocks of the March, 1999 Chamoli earthquake and seismotectonic structure of the Garhwal Himalaya. *Seism. Soc. Amer. Bull.*, v. 93, pp. 109-117.
- Kayal, J.R., Zhao, D., Mishra, O.P., De, R. and Singh, O.P. (2002b) The 2001 Bhuj earthquake: tomography evidence for fluids at hypocentre and its implications for rupture nucleation. *Geophys. Res. Lett.*, v. 29, pp. 51-54.
- Khattri, K.N. and Tyagi, A. K. (1983) Seismicity pattern in the Himalayan plate boundary and identification of the areas of high seismic potential. *Tectonophys.*, v. 96, pp. 281-297.
- Mahadevan, T.M. (1994) Deep continental structure of India: a review. *Geol. Soc. India Mem. No. 28*, 569p
- Martin, S.S. (2005) Intensity distribution from the 2004 M 9.0 Sumatra-Andaman earthquake. *Seism. Res. Lett.*, v. 76, pp. 321-330
- Mishra, D.C., Gupta, S.B. and Vyaghreswara Rao, M.B.S. (1994) Space and time distribution of gravity field in earthquake affected areas of Maharashtra, India. *Geol. Soc. India Mem. No. 35*, pp. 119-126.
- Mishra, O.P., Kayal, J.R., Chakraborty, G.K., Singh, O.P. and Ghosh, D. (2007) Aftershock investigations in the Andaman-Nicobar islands of India and its seismotectonic implications. *Seism. Soc. Amer. Bull.*, v. 97, pp. S71-S85.
- Mukhopadhyay, S. and Kayal J.R. (2003) Seismic tomography structure of the 1999 Chamoli earthquake source area in the Garhwal Himalaya. *Seism. Soc. Amer. Bull.*, v. 93, pp. 1854-1861.
- Ni, J. and Barazangi, M. (1984) Seismotectonics of the Himalayan collision zone: Geometry of the underthrusting Indian Plate beneath the Himalaya *J. Geophys. Res.*, v. 89, pp. 1147-1163.
- Seeber, L., Armbruster, J.G. and Quittmeyer, R. (1981) Seismicity and continental subduction in the Himalayan Arc, In: Gupta, H.K. and Delany, F.M. (Eds.), *Zagros, Hindu Kush, Himalaya, Geodynamic Evolution*. *Geodyn. Ser.*, v. 3, pp. 215-242.
- Valdiya, K.S. (1984) *Aspects of tectonics: Focus on south central Asia*. Tata McGraw Hill Publ. Co. Ltd., New Delhi, 319p.